Laboratory Investigation (2017) 97, 543–554

Maresin1 stimulates alveolar fluid clearance through the alveolar epithelial sodium channel Na,K-ATPase via the ALX/PI3K/Nedd4-2 pathway

Jun-Li Zhang[1], Xiao-Jun Zhuo[1], Jing Lin[1], Ling-Chun Luo[1], Wei-Yang Ying[1], Xiang Xie[1], Hua-Wei Zhang[1], Jing-Xiang Yang[1], Dan Li[1], Fang Gao Smith[1,2] and Sheng-Wei Jin[1]

Maresin1 (MaR1) is a new docosahexaenoic acid-derived pro-resolving agent that promotes the resolution of inflammation. In this study, we sought to investigate the effect and underlining mechanisms of MaR1 in modulating alveolar fluid clearance (AFC) on LPS-induced acute lung injury. MaR1 was injected intravenously or administered by instillation (200 ng/kg) 8 h after LPS (14 mg/kg) administration and AFC was measured in live rats. In primary rat alveolar type II epithelial cells, MaR1 (100 nM) was added to the culture medium with lipopolysaccharide for 6 h. MaR1 markedly stimulated AFC in LPS-induced lung injury, with the outcome of decreased pulmonary edema and lung injury. In addition, rat lung tissue protein was isolated after intervention, and we found MaR1 improved epithelial sodium channel (ENaC), Na, K-adenosine triphosphatase (ATPase) protein expression and Na,K-ATPase activity. MaR1 down-regulated Nedd4-2 protein expression though PI3k/Akt but not though PI3k/SGK1 pathway *in vivo*. In primary rat alveolar type II epithelial cells stimulated with LPS, MaR1-upregulated ENaC and Na,K-ATPase protein abundance in the plasma membrane. Finally, the lipoxin A4 Receptor inhibitor (BOC-2) and PI3K inhibitor (LY294002) not only blocked MaR1's effects on cAMP/cGMP, the expression of phosphorylated Akt and Nedd4-2, but also inhibited the effect of MaR1 on AFC *in vivo*. In conclusion, MaR1 stimulates AFC through a mechanism partly dependent on alveolar epithelial ENaC and Na,K-ATPase activation via the ALX/PI3K/Nedd4-2 signaling pathway. Our findings reveal a novel mechanism for pulmonary edema fluid reabsorption and MaR1 may provide a new therapy for the resolution of ALI/ARDS.
Laboratory Investigation (2017) **97,** 543–554; doi:10.1038/labinvest.2016.150; published online 20 February 2017

Acute respiratory distress syndrome (ARDS), characterized by alveolar edema which impairs gas exchange, is a devastating condition with 35–45% mortality rate.[1,2] However, there is currently no specific pharmacotherapy to reduce injury or enhance resolution in clinical ARDS patients.[3] Hence, innovative therapies are needed to decrease the mortality.[4] Earlier reports have shown that reduced alveolar fluid clearance (AFC) was a characteristic feature of ARDS.[5] As a result, removal of excessive alveolar edema fluid is an important way for effective treatment and better outcome.[6]

AFC represents alveolar filling and clearance.[7] It has been generally believed that epithelial sodium channel (ENaC) is the primary determinant of AFC, a driving force to remove edema fluid from alveolar spaces on the ion transport-dependent mechanism.[8] Na^+ ions enter alveolar typeII epithelial (ATII) cells at the apical surface primarily through amiloride-sensitive sodium channels and are pumped out on the basolateral surface by Na,K-ATPase (sodium pump). This solute transport drives osmotic water transport.[9] ENaC is composed of α, β, and γ subunits. The three subunits of ENaC are all indispensable for efficient AFC.[10] Neonatal α-ENaC gene knockout mice developed respiratory distress and died within 40 h of birth because of failing to clear the alveolar fluid.[11] Na,K-ATPase inhibition with ouabain reduces the short circuit current across alveolar typeII cells, and markedly decreased solute and fluid transport in alveoli.[12] Many studies have shown that angiotensin,[7] Triiodo-L thyronine,[9] Estradiol,[13] enhanced AFC via increasing ENaC activity or increasing Na,K-ATPase activity. However, these have failed to translate positively in human studies.[14] In addition, our

[1]Department of Anesthesia and Critical Care, Second Affiliated Hospital and Yuying Children's Hospital of Wenzhou Medical University, Zhejiang, China and [2]Academic Department of Anesthesia, Critical Care, Pain and Resuscitation, Birmingham Heartlands Hospital, Heart of England NHS Foundation Trust, Birmingham, UK
Correspondence: Professor S-W Jin, MD, PhD, Department of Anesthesia and Critical Care, Second Affiliated Hospital and Yuying Children's Hospital of Wenzhou Medical University, 109 Xueyuan Road, Wenzhou, Zhejiang 325027, China.
E-mail: jinshengwei69@163.com

Received 5 June 2016; revised 26 November 2016; accepted 6 December 2016

previous studies found that intravenous injection β-agonists (salbutamol) reduced extravascular lung water in ARDS patients, but did not improve the clinical outcome.[15–18]

Maresins are novel macrophage mediators with potent anti-inflammatory and pro-resolving actions.[19] They are biosynthesized via 12-lipoxygenase in humans to generate 14 S-hydroperoxydocosa-4Z,7Z,10Z,12E,16Z,19Z-hexaenoic acid, which undergoes further conversion to 13(14)-epoxidation and is subsequently converted to 7,14-dihydroxydocosa-4Z,8Z,10,12,16Z,19Z-hexaenoic acid, known as maresin1 (MaR1).[20] Maresin1 proved to be a potent mediator by stopping polymorphonuclear infiltration and stimulating macrophages phagocytosis.[21,22] Previous data from our group suggested that both resolvin D1 (ref. 23) and lipoxin A4 (ref. 24) activated alveolar epithelial sodium channel, Na, K-ATPase, and increased AFC. However, so far there are no studies about the effects and mechanisms underlying the actions of MaR1 on pulmonary edema.

This study was designed to investigate whether MaR1 could exert protective effects on AFC in LPS-induced ALI. In addition, we investigated the effect of MaR1 on the protein expression of ENaC, Na,K-ATPase, SGK1, Akt and Nedd4-2, and the activity of Na,K-ATPase. Finally, to better understand the mechanisms of action of MaR1, we used ALX receptor inhibitor (BOC-2) and PI3K inhibitor (LY294002) to investigate how this signaling pathway regulated ENaC and AFC.

MATERIALS AND METHODS

Materials

7(R)-MaR1 and LY294002 (PI3K inhibitor) were from Cayman Chemical Company (Ann Arbor, MI, USA). LPS (*Escherichia coli* serotype 055:B5) was purchased from Sigma (St Louis, MO, USA). Myeloperoxidase (MPO), TNF-α, IL-10, cAMP, cGMP ELISA kits were from R&D Systems (Minneapolis, MN, USA). BOC-2 (ALX inhibitor) was obtained from Biomol-Enzo Life Sciences (Farmingdale). Anti-ENaC-α, β, γ, anti-Na,K-ATPase-α1, β1, anti-P-SGK1 (ser^{422}), anti-total-SGK1 were purchased from Abcam (Cambridge, MA, USA). Anti-P-Akt^{473} and anti-total-Akt were purchased from Cell Signalling Technology (Cell Signaling Technology, Danvers, MA, USA).

Animal Preparation

Adult male Sprague–Dawley rats were used to perform experiments (280–320 g, Shanghai Experimental Animal Center of China). The use of animals in this study was approved by the Animal Studies Ethics Committees of the Second Affiliated Hospital of Wenzhou Medical University.

Rats were randomly divided into six groups ($n = 8$): control group, LPS group, LPS+MaR1 (intravenous, i.v.) group, LPS +MaR1 (instill) group, MaR1 (i.v.) group, MaR1 (instill) group. The LPS-induced lung injury model was produced by 14 mg/kg LPS injected via caudal vein. In the MaR1 (i.v.) group or the MaR1 (instill) group, rats received MaR1 (200 ng/kg) i.v. via caudal or via instillation. In other groups, rats received MaR1 or alcohol or equivalent volume of saline (the control group) via caudal vein 8 h after LPS exposure. Animals were anesthetized with an intraperitoneal (i.p.) injection of 5% chloral hydrate (7 mg/kg), after which a tracheotomy tube was placed. Rats were sacrificed after 60 min of mechanical ventilation and lungs were collected.

Pathological Studies

The right lower lung lobes were collected and fixed with 10% neutral-buffered formalin for 24 h, then embedded in paraffin and stained with H&E for light microscope analysis. A semi-quantitative scoring system was adopted to evaluate the lung injury including alveolar congestion, alveolar hemorrhage, infiltration or aggregation of neutrophils in the airspace or vessel wall, and thickness of alveolar wall/hyaline membrane formation and inflammatory cell infiltration. The grading scale to score the pathologic findings was as follows: 0 = no injury; 1 = slight injury (25%); 2 = moderate injury (50%); 3 = severe injury (75%); and 4 = very severe injury (almost 100%). The results were graded from 0 to 4 for each item, as described previously.[25] The four variables were summed to represent the lung injury score (total score: 0–16). Part of the right lung was homogenized from individual rats and centrifuged, and the tissue level of MPO, TNF-α, IL-10 in the resulting supernatants was, respectively, determined using a rat MPO ELISA kit, a rat TNF-α ELISA kit, a rat IL-10 ELISA kit.

Measurement of AFC in Live Rats

AFC was measured in living rats as previously described[9,26,27] with some modifications. Clearance is expressed as a percentage of total instilled volume cleared after 60 min. AFC was determined by Evans blue-tagged albumin concentration changes, which has been clearly characterized by our laboratory.[24]

For preparation of the alveolar instilled solution, a 5% albumin-instilled solution was prepared by dissolving 50 mg/ml BSA in modified lactated Ringer's solution: 137 mM NaCl, 4.67 mM KCl, 1.82 mM $CaCl_2 \times 2H_2O$, 1.25 mM $MgSO_4 \times 7H_2O$, 5.55 mM dextrose, and 12 mM HEPES. The pH was adjusted to 7.4 at 37 °C. The albumin solution was labeled with 0.15 mg/ml Evans blue. In brief, after anesthesia with 5% chloral hydrate (7 ml/kg), a polyethylene endotracheal tube was inserted through a tracheotomy. Rats were ventilated with a constant volume ventilator (model HX-300 Animal ventilators; Taimeng Company of Chengdu, China) with an inspired oxygen fraction of 100%, a respiratory rate of 45–50 breaths per min and 2.86 ± 0.2 ml tidal volumes, positive end expiratory pressure was kept at 2–3 cm H_2O during the baseline period. After tracheotomy, the rats were allowed to stabilize for 10 min. The animals were then placed in the left lateral decubitus position, and instillation tubing (16G Epidural catheter) was gently passed through the tracheotomy tube into the left lung. A total of 1.5 ml (5 ml/kg) of the

instilled solution was instilled at a rate of 0.08 ml/min using a syringe pump. After instillation was complete, 0.2 ml air was injected to clear the instillation catheter of liquid. The instillate remaining in the syringe was collected as the initial sample. After instillation, the catheter was left in place for duration of 60 min. The final alveolar sample was collected via the instillation catheter. The concentrations of Evans blue-labeled albumin in the instilled and aspirated solutions were measured by a spectrophotometer at a wavelength of 621 nm. AFC was calculated using the following equation: $AFC = (1 - C_0/C_1)$, where C_0 is the protein concentration of the instillate before instillation, and C_1 is the protein concentration of the sample obtained at the end of 60 min of mechanical ventilation.

Evaluation of Pulmonary Edema

The lower lobes of the right lung from each group were assessed for dry/wet weight ratios. The remaining lung tissues were collected for further analysis and stored at − 80 °C.

Primary Rat ATII Cells Isolation, Culture, and Treatment

Primary rat ATII cells were isolated from Sprague–Dawley rats (200–250 g) by elastase digestion of lung tissue and then differentially adhered on IgG-coated plates as described by Dobbs *et al.*[28] The purity of ATII cells was assessed by modified Papanicolaou stain based on the presence of dark blue inclusions. Cell viability was assessed by trypan blue exclusion (>95%). ATII cells were seeded onto plastic culture dishes at $1 \times 10^6/cm^2$ and cultured in a 5% CO_2, 95% air atmosphere in DMEM containing 10% FBS, 2 mM L-glutamine, 100 U/ml penicillin, and 0.1 mg/ml streptomycin after isolation. For all experiments, cells were subcultured into six-well plates and maintained until sub-confluence (80%), and cells were serum deprived for 24 h before the addition of LPS (1 μg/ml) in the presence or absence of MaR1 (100 nM).

Western Blotting for ENaC, NaN, K-ATPase, Akt, SGK1, and Nedd4-2

Proteins were obtained with RIPA lysis buffer (50 mM Tris (pH 7.4), 150 mM NaCl, 1% Triton X-100,1% sodium deoxycholate, 0.1% SDS, sodium orthovanadate, sodium fluoride, EDTA, and leupeptin) and PMSF. Samples were ultrasonicated three times, for 5 s, and then spun at 12 000 *g* per min for 30 min. Protein concentrations of the supernatants were determined by using a BCA protein assay kit (Thermo Scientific, Rockford, IL, USA). Proteins were separated by 10% SDS polyacrylamide gels and transferred to PVDF membranes. After blocking with 5% nonfat dried milk in TBS containing 0.05% Tween 20, the membranes were incubated with primary Abs ENaC-α, β, γ (1:500, 1:1000, 1:3000), Na,K-ATPase-α1, β1 (1:1000), and β-actin (internal control, 1:500), Akt (1:2000), SGK1 (1:500), phosphor Akt (1:1000) and phospho SGK1 (1:1000), Nedd4-2 (1:5000) overnight at 4 °C, and then reacted with HRP-conjugated secondary Ab (1:1000; Santa Cruz Company) at room temperature for 1.5 h. The protein bands were detected by ECL and visualized by UVP Gel imaging system (Upland, CA, USA). The band intensity was analyzed by AlphaEaseFC (version 4.0).

Confocal Imaging

ATII cells were respectively treated with saline, LPS (1μg/ml), LPS+MaR1 (100 nM), and MaR1 for 12 h after fixing in 4% paraformaldehyde and blocked with PBS containing 10% donkey serum for 30 min. The cells were then incubated in a 1:50 dilution of monoclonal mouse anti-Na,K-ATPase and goat anti-ENaC-α at 4 °C for 48 h, followed by Alexa Fluor donkey anti-goat and donkey anti-mouse IgG incubation (1:100 and 1:300; Jackson) at room temperature for 2 h. Cell images were acquired with confocal laser-scanning microscope (Leica) and analyzed by Image Pro plus 6.3 software (Media Cybernetics, Q: 13MA).

Measurement of Na,K-ATPase Activity in Rat Lung Tissues

The hydrolytic activity of Na,K-ATPase was measured as ouabain-sensitive ATP hydrolysis under maximal velocity conditions by measuring the release of inorganic phosphate from ATP, as previously described.[29] In brief, the rat lung tissues were digested, subjected to centrifugal sedimentation, lysed, and homogenized. The minimal ATP enzyme test kit (Jiancheng Company, Nanjing, China) was used to assay Na, K-ATPase activity following manufacturer's instructions.

Measurement of cAMP and cGMP Concentrations

cAMP and cGMP concentration in cell lysates and in lung tissue homogenate were measured via ELISA kits according to the manufacturer's instructions.

Statistical Analyses

Data are represented as mean ± s.e.m. All data were analyzed by the Student *t*-test or by one-way ANOVA followed by Tukey's *post-hoc* test for multiple comparisons. Significance was determined at the $P<0.05$ level. Statistical analyses were performed using Prism 5.0 software (GraphPad Software, San Diego, CA, USA).

Results

MaR1 Alleviated LPS-induced ALI

First, we evaluated the effect of MaR1 on LPS-induced ALI. The control group revealed normal pulmonary histology (Figure 1a). Compared with the control group, lung tissues in the LPS group were significantly damaged with interstitial edema, hemorrhage, and inflammatory cells infiltration as evidenced by an increase in lung injury score ($P<0.01$). All the morphologic changes were less pronounced in the LPS +MaR1 (i.v.) group and in the LPS+MaR1 (instill) group. MaR1 significantly attenuated LPS-induced pathologic changes by the evidence of a decrease in lung injury score

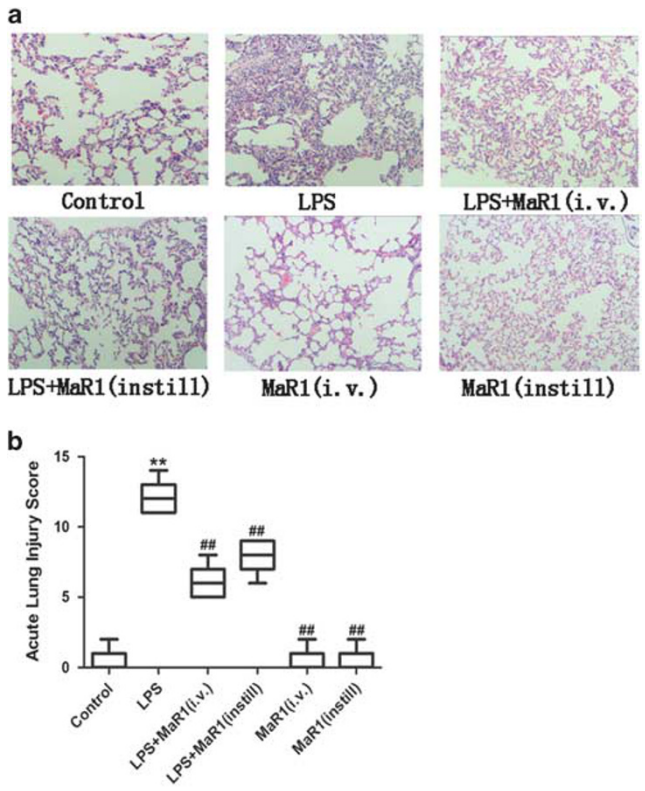

Figure 1 MaR1 protected lung tissues in LPS-induced ALI. MaR1(200ng/kg) was administered to Sprague–Dawley rats 8 h after LPS (14 mg/kg) stimulation through caudal vein or via alveolar instillation, ventilating for 60 min, and the effect of MaR1 was assessed (**a**) by histology in H&E-stained sections (original magnification ×400). Lung injury scores (**b**) were recorded from 0 (no damage) to 16 (maximum damage) according to the criteria described in 'Materials and Methods' section. Data are presented as mean ± s.e.m. $n = 8$. MaR1 (i.v.), intravenous. MaR1 (instill), alveolar instillation. The control group, equivalent volume of saline. $^{**}P < 0.01$ *versus* control group; $^{\#\#}P < 0.01$ *versus* LPS group.

($P < 0.01$). There was no significant difference between the control and MaR1 groups (Figure 1b).

Next, lung tissues homogenate MPO, TNF-α, and IL-10 concentration were analyzed. The concentration of MPO, TNF-α, and IL-10 were significantly increased in the LPS group compared with the control group ($P < 0.01$), but greatly attenuated in the MaR1 treatment group compared with the LPS group ($P < 0.01$; Figures 2a–c).

MaR1-Upregulated AFC in LPS-Induced ALI *In Vivo*

As shown in Figure 3a, the effect of LPS on AFC was dose–response relationship. Next, we examined the effect of MaR1 on AFC in LPS-induced ALI *in vivo*. MaR1 at a concentration of 200 ng/kg was injected through caudal vein or through alveolar instillation 8 h after LPS (14 mg/kg) administration, and AFC was determined after 60 min. AFC in the LPS group was as expected, reduced compared with the control group ($P < 0.01$), whereas MaR1 increased AFC after LPS-challenged ALI ($P < 0.05$ or $P < 0.01$). Moreover, there was significant increase in MaR1 (instill) group ($P < 0.05$ *versus* control group; Figure 3b). In contrast, AFC in the amiloride group was reduced compared with the control group ($P < 0.01$), whereas MaR1 cannot increased AFC after amiloride-challenged ($P < 0.01$; Figure 3c).

MaR1 Attenuated Pulmonary Edema

We examined pulmonary edema by measuring lung wet/dry weight ratios. Figure 4 shows a significant increase in the wet/dry weight ratio in the LPS group compared with the control group ($P < 0.01$). In contrast, the wet/dry ratios in the LPS +MaR1 (i.v.) and LPS+MaR1 (instill) group were lower than the LPS group ($P < 0.01$).

MaR1 Enhanced ENaC in LPS-Induced ALI *In Vivo*

To clarify whether MaR1 effects on AFC are mediated by ENaC, the protein was isolated from rat lungs and measured by western blotting. As shown in Figure 5, the protein expression of ENaC-α and γ subunits in rat lung tissue homogenates were increased in the LPS+MaR1 (i.v.) group compared with the LPS group ($P < 0.01$) and the protein expression of ENaC-γ in rat lung tissue homogenates was increased in the LPS+MaR1 (instill) group compared with the LPS group ($P < 0.01$). However, no significant change in protein expression of ENaC-β subunit was observed after treatment with MaR1 ($P > 0.05$; Figure 5).

MaR1-Upregulated Na,K-ATPase in LPS-Induced ALI *In Vivo*

As shown in Figure 6a, the protein expression of Na,K-ATPase β1 subunit in rat lung tissue homogenates was increased in the LPS+MaR1 (i.v.) group and LPS+MaR1 (instill) group compared with the LPS group ($P < 0.01$). However, no significant change in protein expression of Na, K-ATPase-α1 subunit was observed after treatment with MaR1 ($P > 0.05$; Figure 6a).

As shown in Figure 6b, the Na,K-ATPase activity in the LPS group was markedly decreased compared with the control group ($P < 0.01$), whereas MaR1 augmented Na,K-ATPase activity after LPS-induced ALI ($P < 0.01$).

Dose and Time Dependency MaR1 Regulated Na,K-ATPase-β1 Expression in Primary ATII Cells

Western blotting was used to determine the dose–response and temporal expression patterns relationship of MaR1 regulating Na,K-ATPase-β1 subunit expression. Incubating with the different concentrations of MaR1 including 1, 10, 50, and 100 nM with cells. As shown in Figure 7a, the Na,K-ATPase-β1 subunit expression was increased dose-dependently with a concentration of 100 nM producing a maximal effect. In subsequent experiments, the ENaC and Na,K-ATPase expression in ATII cells was assessed using 100 nM MaR1 (Figure 7a).

In Figure 7b showed the dynamic expression of Na,K-ATPase-β1 subunit in primaryII cells. The expression of Na,

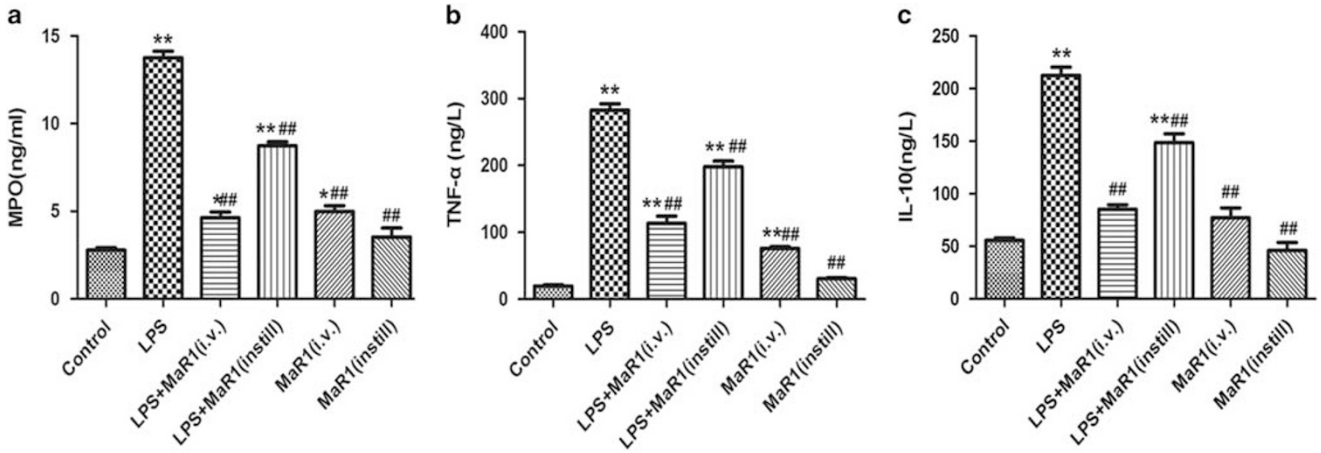

Figure 2 MaR1 regulated the level of inflammatory factors. Lung tissues MPO (**a**), TNF-α (**b**), and IL-10 (**c**) were measured to quantitatively define the resolution of infiltrated cells. Data are presented as mean ± s.e.m. $n = 8$. MaR (i.v.), intravenous. MaR1 (instill), alveolar instillation. The control group, equivalent volume of saline. *$P < 0.05$ *versus* control group; **$P < 0.01$ *versus* control group; $^{\#\#}P < 0.01$ *versus* LPS group.

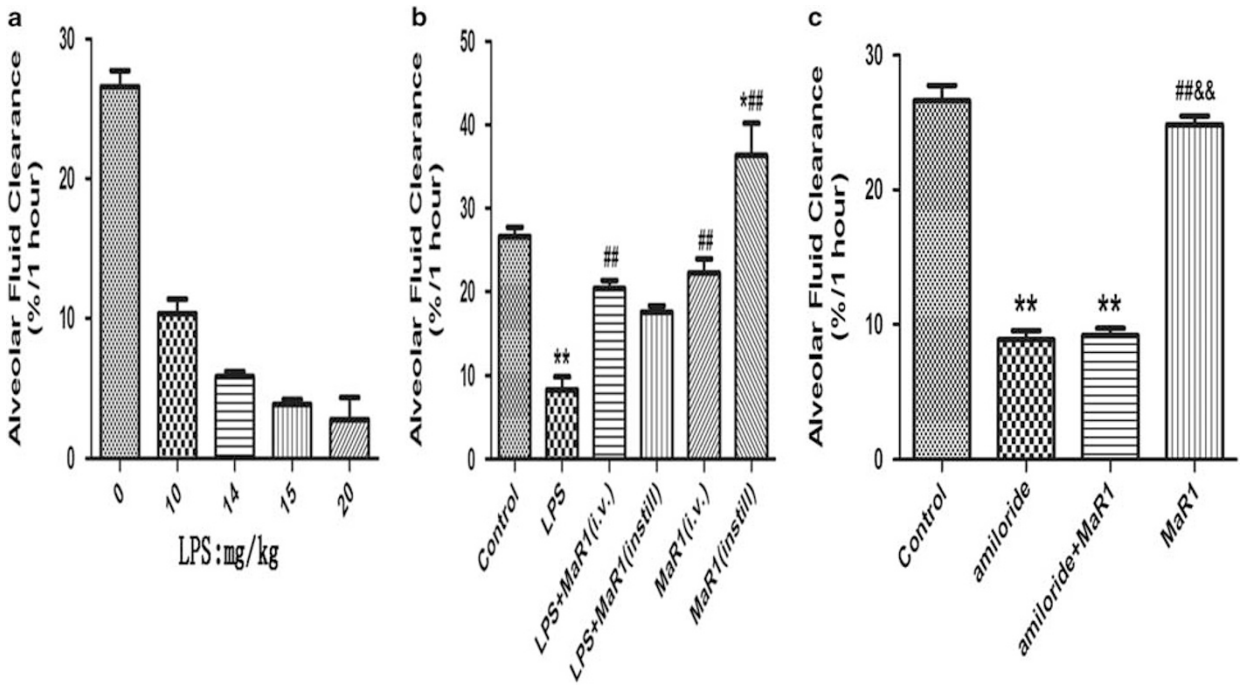

Figure 3 MaR1-upregulated AFC in LPS-induced ALI *in vivo*. MaR1(200 ng/kg) was administered to Sprague–Dawley rats 8 h after LPS (14 mg/kg) stimulation through caudal vein or via alveolar instillation, ventilating for 60 min. Dose dependency of LPS-regulated AFC (**a**). MaR1-upregulated AFC (**b**). ENaC inhibitor experiments (**c**). Data are presented as mean ± s.e.m. $n = 8$. MaR1 (i.v.), intravenous. MaR1 (instill), alveolar instillation. The control group, equivalent volume of saline. *$P < 0.05$ *versus* control group, **$P < 0.01$ *versus* control group; $^{\#}P < 0.05$ *versus* LPS group, $^{\#\#}P < 0.01$ *versus* LPS group.

K-ATPase-β1 subunit was significantly increased at 1 h ($P < 0.01$).

MaR1 Increased ENaC and Na,K-ATPase Protein Abundance in the Plasma Membrane in Primary ATII Cells

Confocal laser-scanning microscopy further examined the effect of MaR1 on the subcellular distribution of the ENaC-α and Na,K-ATPase-α. MaR1 significantly increased ENaC-α abundance in the plasma membrane compared with the LPS group (Figure 8a). Moreover, MaR1 significantly increased Na,K-ATPase-α abundance in the plasma membrane compared with the LPS group (Figure 8b). These results of microscopic images were consistent with immunohistochemistry of rat lung tissues.

MaR1-Induced cAMP and cGMP Elevation Stimulated with LPS *In Vivo* and *Vitro* was Dependent on ALX

To test whether MaR1 (100 nM) has an impact on cAMP and cGMP levels in ATII cells, we measured cAMP and cGMP

concentration in primary ATII cells stimulated with LPS (1 μg/ml) for 6 h by ELISA kits. We found the concentration of cAMP and cGMP in the LPS group was significantly decreased ($P<0.01$) than the control group, however MaR1 treatment significantly increased the concentration of cAMP and cGMP compared with the LPS group ($P<0.01$; Figures 9a and b). To further test whether MaR1 has an impact on cAMP and cGMP levels, we measured cAMP and cGMP concentration in lung tissues. We found cAMP and cGMP concentration were decreased in the LPS group compared with the control group ($P<0.01$), and MaR1 treatment abrogated the increased cAMP and cGMP concentration compared with the LPS group ($P<0.01$). In addition, cAMP and cGMP concentration were decreased in the LPS+MaR1+BOC-2 group compared with the LPS+MaR1 group ($P<0.01$), but not decreased in the LPS+MaR1 +LY294002 group ($P>0.05$; Figures 9c and d).

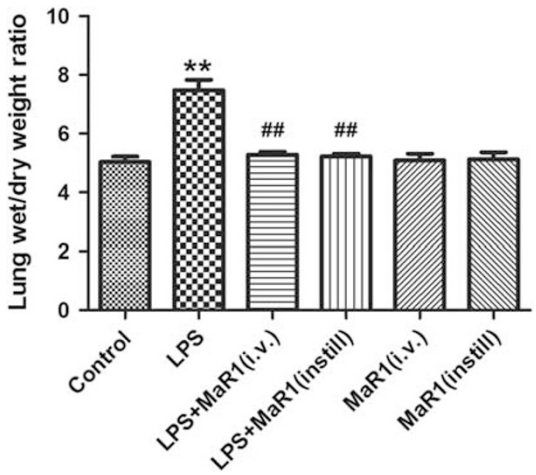

Figure 4 MaR1 attenuated pulmonary edema. MaR1 (200 ng/kg) was administered to Sprague–Dawley rats 8 h after LPS (14 mg/kg) stimulation through caudal vein or via alveolar instillation, ventilating for 60 min. Lung wet/dry weight ratio.

MaR1 Promoted AFC Through Activating the ALX/PI3K Pathway *In Vivo*

To further investigate ALX/PI3K-dependent actions of MaR1 *in vivo*, we co-administered MaR1 (200 ng/kg) and BOC-2 (600 ng/kg) or LY294002 (3 mg/kg) to Sprague–Dawley rats through caudal vein 8 h after LPS (14 mg/kg) administration, and AFC was determined after 60 min. As shown in Figure 10c, AFC was markedly reduced in the LPS group compared with the control group ($P<0.01$), whereas MaR1 treatment group markedly increased AFC compared with the LPS group ($P<0.01$). However, AFC in the LPS+MaR1 +BOC-2 and LPS+MaR1+LY294002 groups was markedly reduced compared with the MaR1 treatment group ($P<0.01$).

MaR1 Regulated Nedd4-2 Through Activating PI3k/Akt pathway not PI3k/SGK1 Pathway *In Vivo*

To further investigate whether MaR1 regulate Nedd4-2 via PI3k/Akt pathway or PI3k/SGK1 pathway. The protein expression of Ser^{473}-phos-phorylated Akt and ser^{422}-phos-phorylated SGK1 in rat lung tissue homogenates were measured by western blotting. The protein level of phos-phorylated Akt in the LPS group was markedly decreased compared with control group ($P<0.01$) and markedly increased in the LPS+MaR1 group compared with the LPS group ($P<0.01$). BOC-2 and LY294002 markedly suppressed the MaR1-induced increased in the protein level of

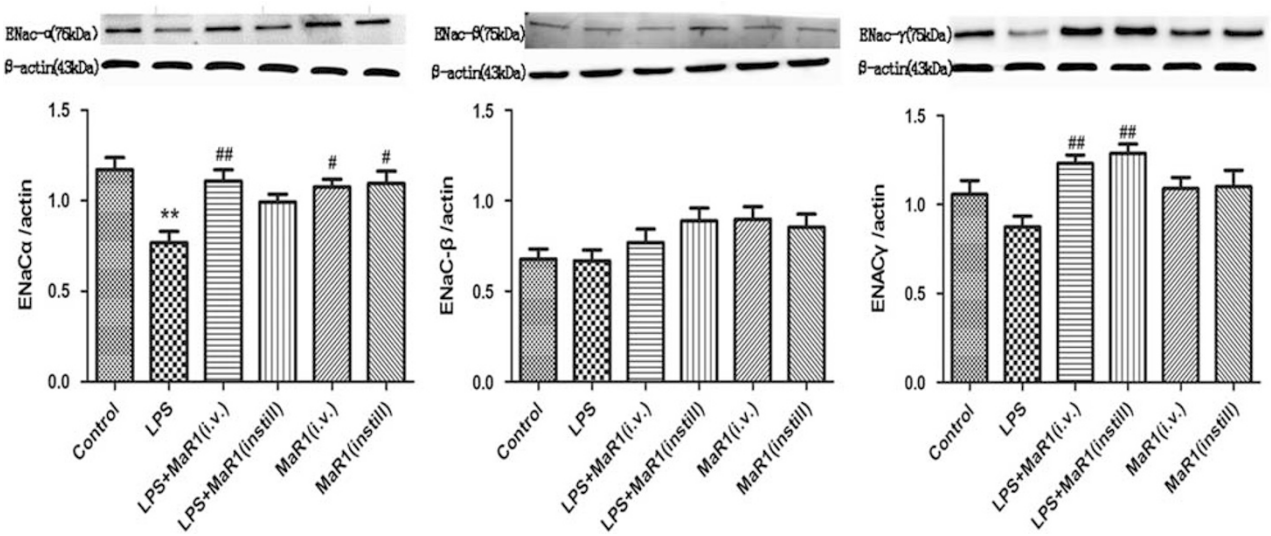

Figure 5 MaR1 enhanced ENaC expression by western blotting in LPS-induced ALI *in vivo*. MaR1(200 ng/kg) was administered to Sprague–Dawley rats 8 h after LPS (14 mg/kg) stimulation through caudal vein or via alveolar instillation, ventilating for 60 min, and the right lung tissue was collected to measure the protein expression of ENaC-α, β, and γ subunits by western blotting. Western blot data were replicated >3 times. The control group, equivalent volume of saline. Data are presented as mean ± s.e.m. $n=8$. $^{**}P<0.01$ *versus* control group; $^{\#}P<0.05$, $^{\#\#}P<0.01$ *versus* LPS group.

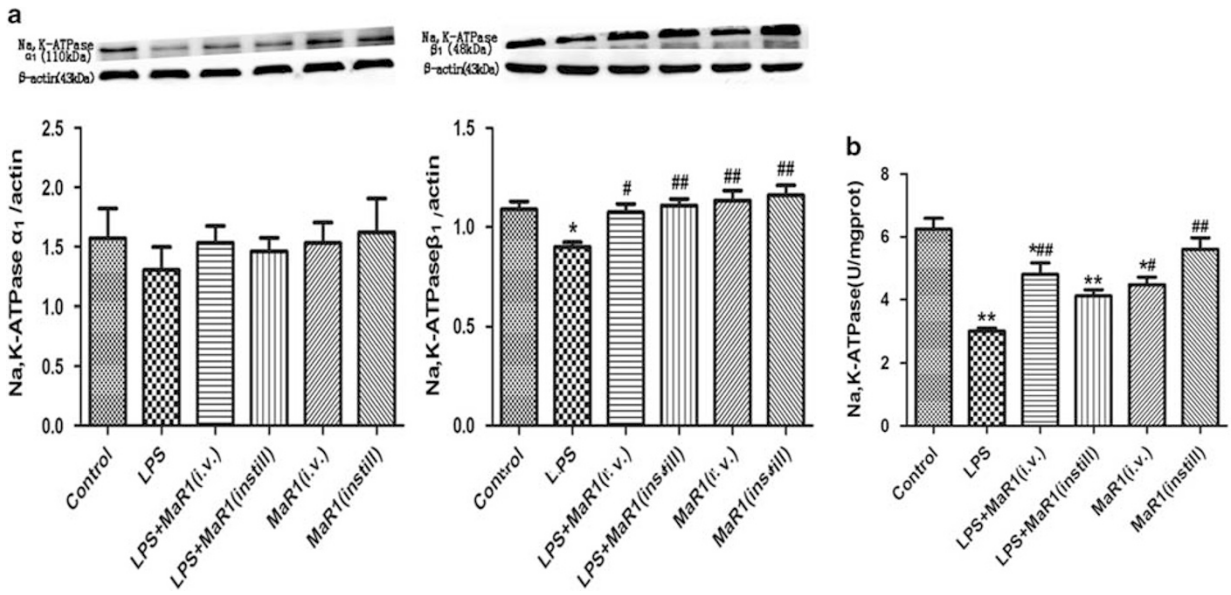

Figure 6 MaR1 enhanced Na,K-ATPase expression by western blotting and Na,K-ATPase activity in LPS-induced ALI *in vivo*. MaR1 (200 ng/kg) was administered to Sprague–Dawley rats 8 h after LPS (14 mg/kg) stimulation through caudal vein or via alveolar instillation, ventilating for 60 min, and the right lung tissue was collected to measure the protein expression of Na,K-ATPase-α1 and β1 subunits by western blotting (**a**). Western blot data were replicated >3 times and the Na,K-ATPase activity in lung tissue homogenate was detected by kits (**b**). The control group, equivalent volume of saline. Data are presented as mean ± s.e.m. $n=8$. $^{*}P<0.05$, $^{**}P<0.01$ *versus* control group; $^{\#}P<0.05$, $^{\#\#}P<0.01$ *versus* LPS group.

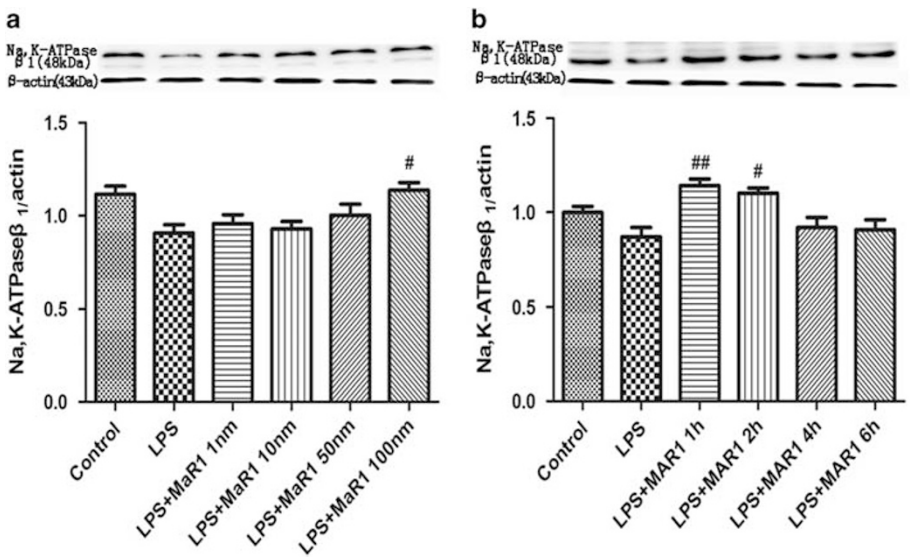

Figure 7 Dose and time dependency of MaR1 regulated Na,K-ATPase expression in primary ATII cells. The dose- and temporal-dependent changes of Na,K-ATPase protein expression in primary ATII cells stimulated with LPS (1μg/ml) were determined by western blotting. Western blot data were replicated >3 times. Cells were incubated with different concentrations of MaR1 for 6 h including 1, 10, 50, and 100 nM to measure the Na,K-ATPase-β1 subunit protein expression (**a**). Moreover, ATII cells were incubated with LPS (1 μg/ml) for 1, 2, 4, and 6 h to detect the expression of Na,K-ATPase-β1 subunit protein (**b**). $^{\#}P<0.05$, $^{\#\#}P<0.01$ *versus* LPS group.

phosphorylated Akt ($P<0.01$; Figure 10a). Nevertheless, no significant change in the protein level of phosphorylated SGK1 was observed (Figure 10b).

Nedd4-2, an E3 ubiquitin-protein ligase, is critical in the negative control of Na^+ transport. To further investigated the effect of MaR1 on Nedd4-2, the protein expression of Nedd4-2 in rat lung tissue homogenates was measured by western blotting. The protein level of Nedd4-2 in LPS group was significantly increased compared with the control group ($P<0.05$) and significantly decreased in the MaR1 treatment group compared with the LPS group ($P<0.05$). However, the protein level of Nedd4-2 in LPS+MaR1+BOC-2 group and in LPS+MaR1+LY294002 group was significantly increased compared with the LPS+MaR1 group (Figure 10d).

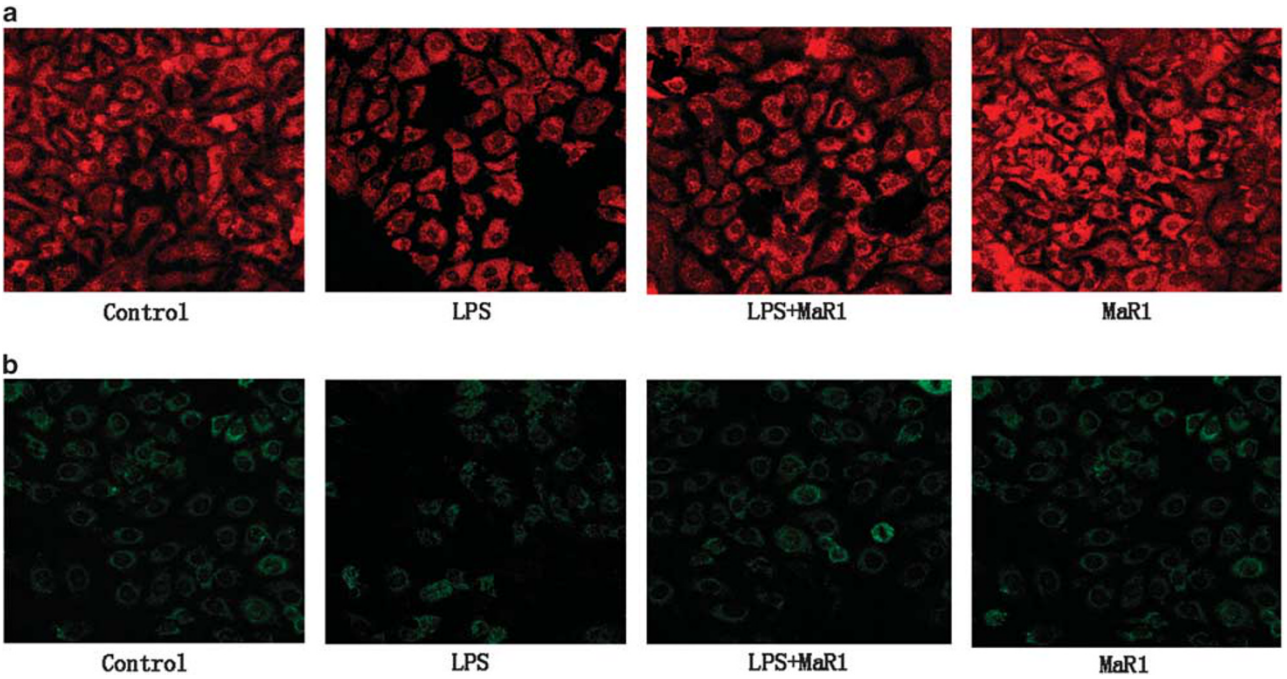

Figure 8 MaR1 increased ENaC and Na,K-ATPase protein abundance in the plasma membrane in primary ATII cells stimulated with LPS. Rat primary ATII cells were treated with MaR1 (100 nM) in the presence or absence of LPS (1 μg/ml) for 6 h. The effect of MaR1 on the subcellular distribution of the ENaC-*α* (**a**) and Na,K-ATPase-*α* (**b**) were examined by confocal laser-scanning microscopy using a specific Ab against (original magnification ×400). Alexa Fluor second Ab was used to stain the cells.

DISCUSSION

In this study, we provide evidence for the pro-resolution activity of MaR1 in ARDS. Treatment with MaR1 improved AFC and decreased pulmonary edema and lung injury in LPS-induced ALI in rats. MaR1 most potently regulated AFC with up-regulating the protein expression of ENaC and Na,K-ATPase increasing the activity of Na,K-ATPase *in vivo* and *in vitro*. MaR1 enhanced the subcellular distribution of ENaC and Na,K-ATPase, specifically localized to the apical and basal membrane of the alveolar epithelium. Moreover, BOC-2 and LY294002 blocked the increased AFC response to MaR1. MaR1-induced decrease Nedd4-2 was blocked with BOC-2 and LY294002 treatment, respectively, *in vivo*, indicating MaR1 increased ENaC and Na,K-ATPase expression to promote AFC via the ALX/PI3K/Nedd4-2 signaling pathway.

Acute lung injury is characterized by the disruption of the alveolar epithelial barrier, which results in increased edema formation, as well as impaired edema clearance.[30] It is widely accepted that resolution of alveolar edema is associated with improved oxygenation, shorter duration of mechanical ventilation, and increased likelihood of survival.[31,32] Our data clearly demonstrate that MaR1 significantly attenuated pulmonary edema and improved the air–blood barrier. Furthermore, MaR1 both administered intratracheally and intravenously enhance the rate of AFC 8 h after LPS challenge with the outcome of decreased pulmonary edema, suggesting that MaR1 has a role in the resolution of inflammation. Interestingly, MaR1 has no influence on AFC when administered intravenously, but improved AFC when administrated intratracheally in healthy intact rats. Our results demonstrated that ENaC inhibitor totally abolished the effects of MaR1 indicating ENaC was major mechanism of MaR1. However, our results showed instilled MaR1 had no effect on the protein expression of ENaC and Na,K-ATPase, the mechanisms were under investigated.

The primary force driving fluid reabsorption from the alveolar space into the interstitium and the pulmonary circulation is active Na^+ transport, which leads to an osmotic gradient that drives the movement of fluid from the alveolar space back into the interstitium and eventually to the blood circulation.[33] Several observations confirm that transepithelial sodium transport has a major role in the clearance of fluid from the airspace.[30] In our study, MaR1 not only enhanced lung tissues homogenate ENaC protein expression in LPS-induced ALI, but also increased ENaC protein abundance in the plasma membrane in primary ATII cells stimulated with LPS. Consistent with our findings, similar results have shown that upregulation of ENaC increased pulmonary edema fluid reabsorption and reduced ENaC expression delayed reabsorption of fluid during pulmonary edema after thiourea–induced lung injury.[32,34] These findings, therefore, suggest that MaR1 promotes AFC through upregulation of ENaC protein expression, and increasing EnaC protein abundance in the plasma membrane.

The sodium pump (Na,K-ATPase) located on the basolateral surface of the alveolar epithelial cell transports ions by

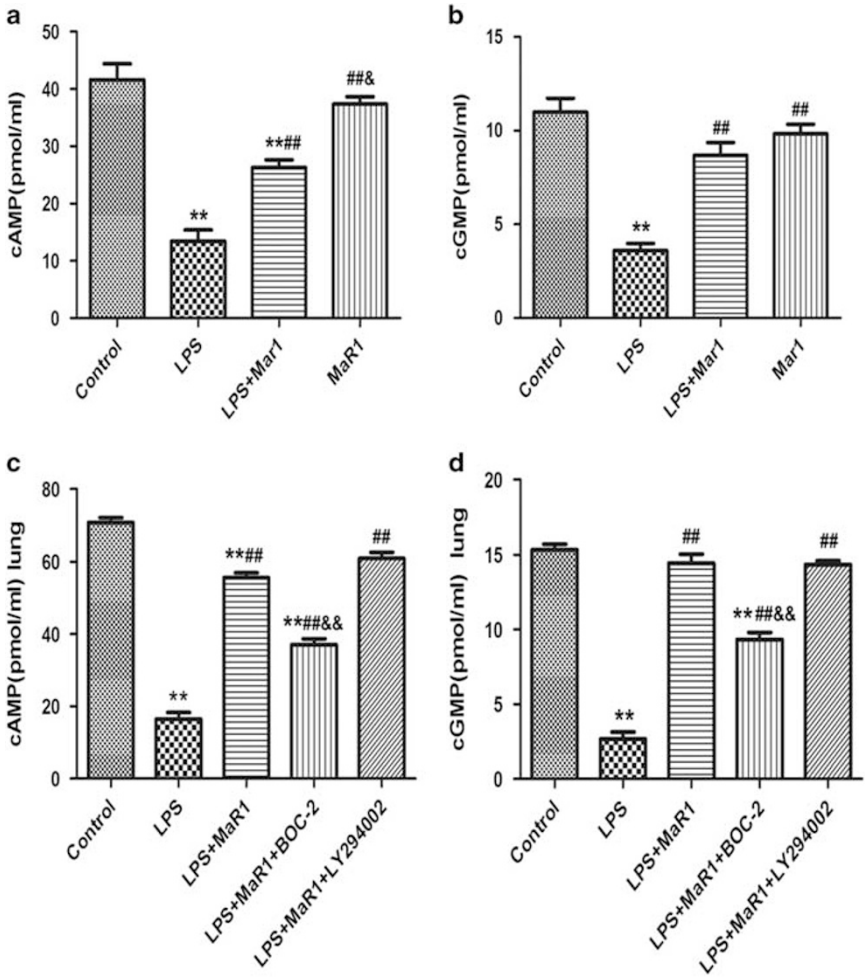

Figure 9 MaR1 increased the concentration of cAMP and cGMP *in vivo* and *vitro*. Primary ATII cells were incubated with MaR1 (100 nm) in the presence of LPS (1 μg/ml) for 6 h. After incubation, the cells were collected and sonicated. cAMP (**a**) and cGMP (**b**) concentration in the cell lysates was detected by ELISA. MaR1 (200 ng/kg) and BOC-2 (ALX receptor inhibitor), LY294002(PI3K inhibitor) were coadministeredto Sprague–Dawley rats 8 h after LPS (14 mg/kg) stimulation through caudal vein, ventilating for 60 min, cAMP (**c**) and cGMP (**d**) concentration in the right lung tissue was detected by ELISA kits. Data are presented as mean ± s.e.m. $n = 8$. $^{**}P < 0.01$ *versus* control group; $^{\#\#}P < 0.01$ *versus* LPS group; $^{\&}P < 0.05$, $^{\&\&}P < 0.01$ *versus* LPS+MaR1 group.

consuming ATP and pumping Na^+ out of the cell in exchange for potassium influx to maintain Na^+ and potassium gradients across the plasma membrane.[35] The basolateral membrane location of the Na,K-ATPase is crucial for alveolar fluid reabsorption where the vectorial Na^+ transport is followed by water in an isosmolar manner.[14,30,36] It has been well established that upregulation of ENaC and Na,K-ATPase increases active Na^+ transport, leading to increased ability of the lungs to clear edema.[30,37] Impairment of Na,K-ATPase function appears to be a hallmark during lung injury even in a preclinical stage.[30,35,38] In our study, we demonstrated that MaR1 not only increased Na,K-ATPase expression in rat lung tissues and primary ATII cells after LPS challenge by western blotting, immunohistochemistry, and confocal laser-scanning microscopy measurement, but also upregulation of Na,K-ATPase activity *in vivo*. Altogether, our data from the lung tissues and cell culture indicate that MaR1 promotes AFC through both of the essential mechanisms of ENaC and Na,K-ATPase.

Specialized pro-resolving lipid mediators (SPMs) derived fromv-3 polyunsaturated fatty acids orchestrate resolution in diverse settings of acute inflammation.[39] Maresin1 is one of family of SPMs displaying potent anti-inflammatory and pro-resolving actions.[21,40] However, so far the receptors and downstream signalling pathways of MaR1 are under investigated. It has been generally believed that the SPMs exert their actions by interacting with G-protein-coupled receptor (GPCR) with high affinity and stereospecificity.[22,41] ALX (lipoxin A4 receptor) is a GPCR with cell-type-specific signaling pathways.[42,43]cAMP and cGMP are important second messengers by which cells extracellular signals into intracellular responses.[23] Extracellular signals interact with GPCRs to activate the AC and increase the intracellular cAMP and cGMP levels. A previous study showed that LPS-induced

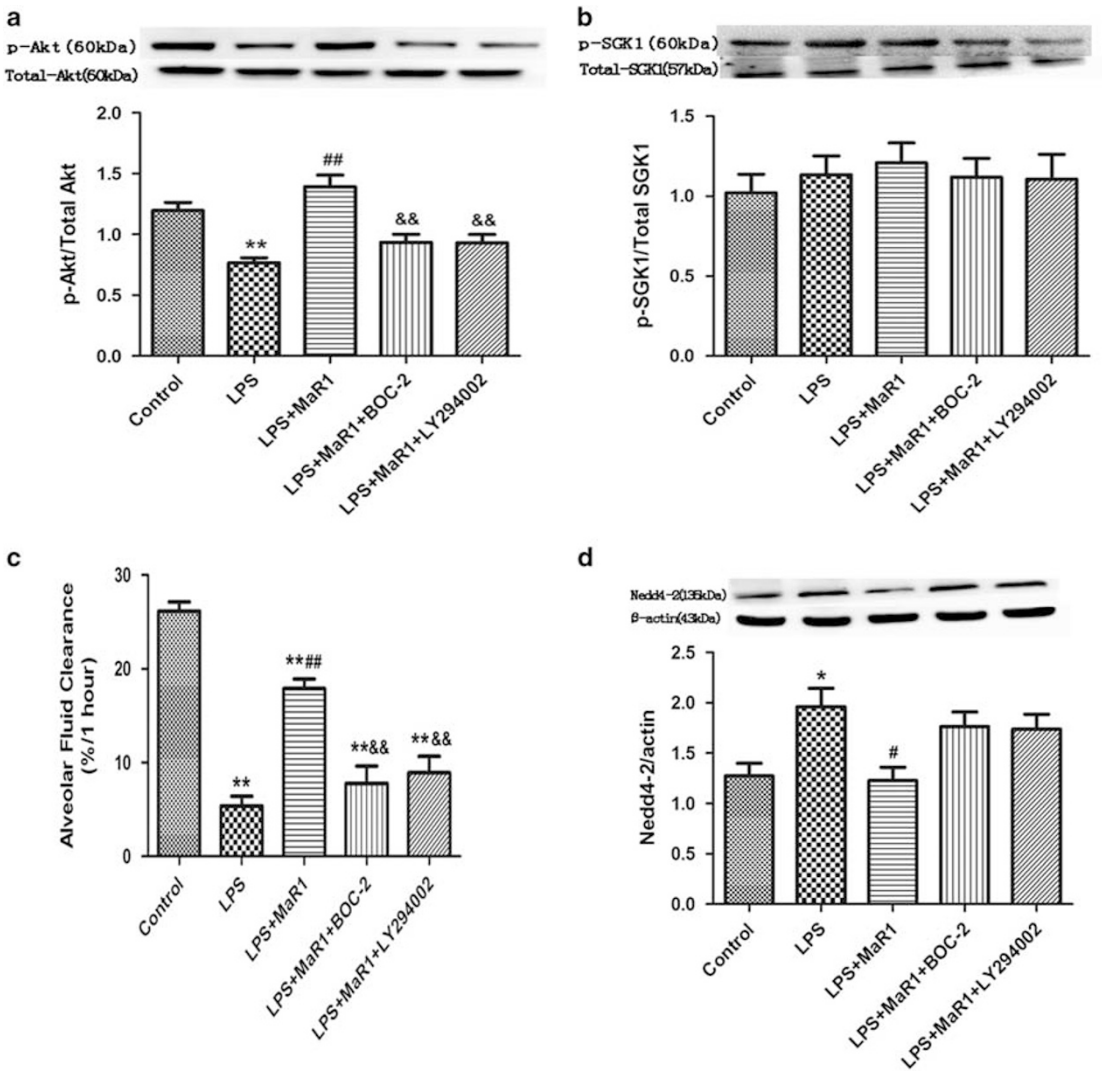

Figure 10 MaR1 improved AFC through activating the ALX/PI3K /AKT/Need4-2 pathway *in vivo*. MaR1 (200 ng/kg) and BOC-2 (600ng/kg), LY294002 (3 mg/kg) were co-administered to Sprague–Dawley rats through caudal vein 8 h after LPS (14 mg/kg) was administered, and intratracheal instillation of 5% albumin solution containing Evans Blue-labeled albumin (5 ml/kg) through a tracheostomy to the left lung; AFC was measured over 60 min in ventilated animals (**c**). Expression of phosphorylated Akt and phosphorylated SGK1 in rat lung 8 h after LPS-induced actue lung injury or saline treatment were measured by western blotting. Western blot data were replicated >3 times. The band intensity of phosphorylated Akt (**a**) and phosphorylated SGK1 (**b**) were quantitated by normalized for total Akt and total SGK1, respectively, and expressed as fold of the control. Expression of Nedd4-2 in rat lung 8 h after LPS-induced acute lung injury or saline treatment were measured by western blotting. Western blot data were replicated >3 times. The band intensity of Nedd4-2 quantitated by normalized for β-actin and expressed as fold of the control (**d**). Data are presented as mean ± s.e.m. $n=8$. $^{**}P<0.01$ *versus* control group; $^{\#\#}P<0.01$ *versus* LPS group; $^{\&\&}P<0.01$ *versus* LPS+MaR1 group.

immune response leads to a decrease of intracellular cAMP.[44] Another study pointed out cGMP-activated Na^+ channels is a novel pathway for resolving fluid in injured lungs.[45,46] Against this background, our purpose was to evaluate whether the role of MaR1 on lung is ALX/cAMP/cGMP dependent. Our studies illustrated that the intracellular cAMP and cGMP level was decreased after LPS stimulation, and MaR1 abrogated the decrease observed in the LPS group *in vitro* and *in vitro*. Furthermore, we found that MaR1-induced increase in the levels of cAMP and cGMP were blocked with BOC-2 (ALX antagonist), not with LY294002 (PI3K inhibitor). Moreover, BOC-2 blocked the increased AFC in MaR1 treatment group. These results, taken together, suggest that the MaR1 response is ALX/cAMP/cGMP dependent.

It is well-known that PI3K signals are implicated in regulating ENaC trafficking and activity.[47] The PI3K has been identified for regulation of ENaC-mediated AFC by insulin.[8] The signaling cascade downstream of PI3K involves of several effector proteins. One is Akt, which is believed to be the central mediator of signaling with profound effects on several physiological events.[48,49] The other candidate for the effector proteins downstream of PI3K that regulate ENaC is SGK. This

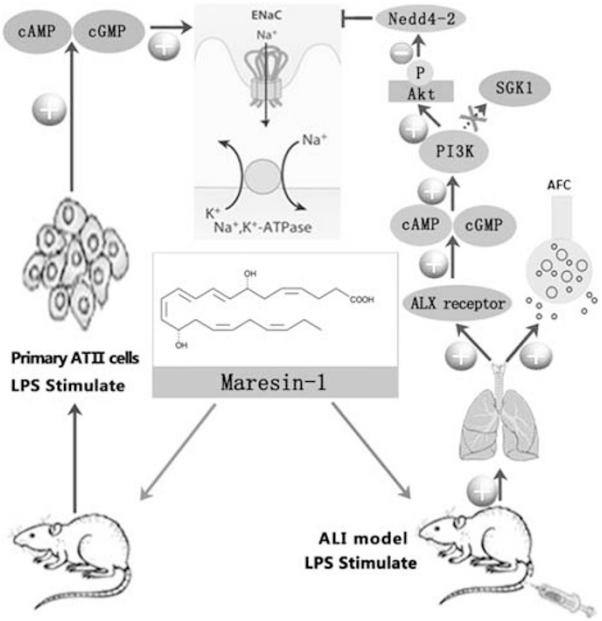

Figure 11 MaR1 protected LPS-induced ALI *in vivo* and *in vitro*.

kinase is known to be a key mediator of the effect of the hormone aldosterone on ENaC.[50] Our studies revealed that p-Akt (ser^{473}) was decreased after LPS stimulation and MaR1 reversed the decreased of p-Akt (ser^{473}), but the beneficial effects were abrogated by BOC-2 and LY294002. However, MaR1 had no effect on the expression of SGK1 (ser^{422}). Furthermore, LY294002 blocked AFC stimulated by MaR1. The implication for our work is that MaR1 promoted AFC by activating p-Akt via PI3K but not p-SGK1.

Nedd4-2, an E3 ubiquitin-protein ligase, which has been shown to negatively regulate ENaC expression *in vitro* and *in vivo*.[51,52] Recent studies using Nedd4-2-deficient mice clearly demonstrated that Nedd4-2, which is co-expressed with ENaC in lung epithelial cells transporting Na^+, has a crucial role in the regulation of ENaC activity in the lung.[53] It was shown that AKT increases ENaC activity by phosphorylation of Nedd4-2, thereby reducing the affinity of Nedd4-2 to ENaC.[49] One study indicated that reducing the ENaC/Nedd4-2 interaction results in an increase in the open probability of the channel.[54] Another study revealed that phosphorylation of Nedd4-2 by Akt reduces the ability of Nedd4-2 to suppress surface expression of ENaC, consequently allowing Na^+ absorption to increase.[48] Consistently, we also found MaR1 inhibited the increase of Nedd4-2 protein expression induced by LPS, the beneficial effect of MaR1 on reducing Nedd4-2 protein expression was abolished by BOC-2 and LY294002 *in vivo*. The results show that the MaR1 response is ALX/ PI3K/Nedd4-2 dependent. The key role for MaR1 during LPS-induced ALI *in vivo* and *in vitro* is summarized in Figure 11.

In conclusion, these data demonstrate that MaR1 alleviated pulmonary edema, enhanced AFC, and attenuated lung injury partially through stimulation of ENaC and Na,K-ATPase via activation of the ALX/PI3K/Nedd4-2 pathway in LPS-induced ALI. Thus, treatment with MaR1 in critically ill patients with ALI has the potential to augment lung edema clearance. More importantly, MaR1 is endogenous chemical mediators during the resolution of inflammation. So, it maybe has fewer side effects. Our findings reveal a novel mechanism for pulmonary edema fluid reabsorption and MaR1 may provide a new therapy for the resolution of ALI/ARDS.

ACKNOWLEDGMENTS

We thank Hong-Xia Mei, Li-Dan Zheng, and Hui Li for assistance with this study. This work was sponsored by the grants from the National Natural Science Foundation of China (Nos. 81570076, 81270132, and 81070061).

DISCLOSURE/CONFLICT OF INTEREST

The authors declare no conflict of interest.

1. Lin EH, Chang HY, Yeh SD, *et al.* Polyethyleneimine and DNA nanoparticles-based gene therapy for acute lung injury. Nanomedicine 2013;9:1293–1303.
2. Peters DM, Vadasz I, Wujak L, *et al.* TGF-beta directs trafficking of the epithelial sodium channel ENaC which has implications for ion and fluid transport in acute lung injury. Proc Natl Acad Sci USA 2014;111: E374–E383.
3. Shyamsundar M, McAuley DF, Ingram RJ, *et al.* Keratinocyte growth factor promotes epithelial survival and resolution in a human model of lung injury. Am J Respir Crit Care Med 2014;189:1520–1529.
4. Li J, Huang S, Wu Y, *et al.* Paracrine factors from mesenchymal stem cells: a proposed therapeutic tool for acute lung injury and acute respiratory distress syndrome. Int Wound J 2014;11:114–121.
5. Tamarapu Parthasarathy P, Galam L, Huynh B, *et al.* MicroRNA 16 modulates epithelial sodium channel in human alveolar epithelial cells. Biochem Biophys Res Commun 2012;426:203–208.
6. Eaton DC, Chen J, Ramosevac S, *et al.* Regulation of Na+ channels in lung alveolar type II epithelial cells. Proc Am Thorac Soc 2004;1:10–16.
7. Deng J, Wang DX, Deng W, *et al.* The effect of endogenous angiotensin II on alveolar fluid clearance in rats with acute lung injury. Can Respir J 2012;19:311–318.
8. Deng W, Li CY, Tong J, *et al.* Regulation of ENaC-mediated alveolar fluid clearance by insulin via PI3K/Akt pathway in LPS-induced acute lung injury. Respir Res 2012;13:29.
9. Bhargava M, Runyon MR, Smirnov D, *et al.* Triiodo-L-thyronine rapidly stimulates alveolar fluid clearance in normal and hyperoxia-injured lungs. Am J Respir Crit Care Med 2008;178:506–512.
10. Downs CA, Kreiner LH, Trac DQ, *et al.* Acute effects of cigarette smoke extract on alveolar epithelial sodium channel activity and lung fluid clearance. Am J Respir Cell Mol Biol 2013;49:251–259.
11. Bardou O, Prive A, Migneault F, *et al.* K+ channels regulate ENaC expression via changes in promoter activity and control fluid clearance in alveolar epithelial cells. Biochim Biophys Acta 2012;1818:1682–1690.
12. Berthiaume Y, Matthay MA. Alveolar edema fluid clearance and acute lung injury. Respir Physiol Neurobiol 2007;159:350–359.
13. Qi D, He J, Wang D, *et al.* 17beta-estradiol suppresses lipopolysaccharide-induced acute lung injury through PI3K/Akt/SGK1 mediated up-regulation of epithelial sodium channel (ENaC) *in vivo* and *in vitro*. Respir Res 2014;15:159.
14. Dushianthan A, Grocott MP, Postle AD, *et al.* Acute respiratory distress syndrome and acute lung injury. Postgrad Med J 2011;87:612–622.
15. Perkins GD, Gao F, Thickett DR. *In vivo* and *in vitro* effects of salbutamol on alveolar epithelial repair in acute lung injury. Thorax 2008;63: 215–220.
16. Sakuma T, Folkesson HG, Suzuki S, *et al.* Beta-adrenergic agonist stimulated alveolar fluid clearance in *ex vivo* human and rat lungs. Am J Respir Crit Care Med 1997;155:506–512.
17. Perkins GD, Park D, Alderson D, *et al.* The beta agonist lung injury Trlal (BALTI)—prevention trial protocol. Trials 2011; 12.

18. Perkins GD, McAuley DF, Thickett DR, *et al.* The beta-agonist lung injury trial (BALTI) - A randomized placebo-controlled clinical trial. Am J Respir Crit Care Med 2006;173:281–287.
19. Serhan CN, Yang R, Martinod K, *et al.* Maresins: novel macrophage mediators with potent antiinflammatory and proresolving actions. J Exp Med 2009;206:15–23.
20. Marcon R, Bento AF, Dutra RC, *et al.* Maresin 1, a proresolving lipid mediator derived from omega-3 polyunsaturated fatty acids, exerts protective actions in murine models of colitis. J Immunol 2013;191:4288–4298.
21. Serhan CN, Dalli J, Karamnov S, *et al.* Macrophage proresolving mediator maresin 1 stimulates tissue regeneration and controls pain. FASEB J 2012;26:1755–1765.
22. Serhan CN. Novel lipid mediators and resolution mechanisms in acute inflammation: to resolve or not? Am J Pathol 2010;177:1576–1591.
23. Wang Q, Zheng X, Cheng Y, *et al.* Resolvin D1 stimulates alveolar fluid clearance through alveolar epithelial sodium channel, Na,K-ATPase via ALX/cAMP/PI3K pathway in lipopolysaccharide-induced acute lung injury. J Immunol 2014;192:3765–3777.
24. Wang Q, Lian QQ, Li R, *et al.* Lipoxin A(4) activates alveolar epithelial sodium channel, Na,K-ATPase, and increases alveolar fluid clearance. Am J Respir Cell Mol Biol 2013;48:610–618.
25. Mikawa K, Nishina K, Takao Y, *et al.* ONO-1714, a nitric oxide synthase inhibitor, attenuates endotoxin-induced acute lung injury in rabbits. Anesth Analg 2003;97:1751–1755.
26. Bellmeyer A, Martino JM, Chandel NS, *et al.* Leptin resistance protects mice from hyperoxia-induced acute lung injury. Am J Respir Crit Care Med 2007;175:587–594.
27. Sakuma T, Zhao Y, Sugita M, *et al.* Malnutrition impairs alveolar fluid clearance in rat lungs. Am J Physiol Lung Cell Mol Physiol 2004;286: L1268–L1274.
28. Dobbs LG, Williams MC, Gonzalez R. Monoclonal antibodies specific to apical surfaces of rat alveolar type I cells bind to surfaces of cultured, but not freshly isolated, type II cells. Biochim Biophys Acta 1988;970: 146–156.
29. Jiang X, Ingbar DH, O'Grady SM. Adrenergic regulation of ion transport across adult alveolar epithelial cells: effects on Cl- channel activation and transport function in cultures with an apical air interface. J Membr Biol 2001;181:195–204.
30. Sartori C, Matthay MA. Alveolar epithelial fluid transport in acute lung injury: new insights. Eur Respir J 2002;20:1299–1313.
31. Matthay MA, Robriquet L, Fang X. Alveolar epithelium: role in lung fluid balance and acute lung injury. Proc Am Thorac Soc 2005;2:206–213.
32. Vadasz I, Raviv S, Sznajder JI. Alveolar epithelium and Na,K-ATPase in acute lung injury. Intensive Care Med 2007;33:1243–1251.
33. Zemans RL, Matthay MA. Bench-to-bedside review: the role of the alveolar epithelium in the resolution of pulmonary edema in acute lung injury. Crit Care 2004;8:469–477.
34. Jiang L, Wang J, Su C, *et al.* α-ENaC, a therapeutic target of dexamethasone on hydrogen sulfide induced acute pulmonary-edema. Environ Toxicol Pharmacol 2014;38:616–624.
35. Matthay MA, Clerici C, Saumon G. Invited review: Active fluid clearance from the distal air spaces of the lung. J Appl Physiol 2002;93:1533–1541.
36. Mutlu GM, Sznajder JI. Mechanisms of pulmonary edema clearance. Am J Physiol Lung Cell Mol Physiol 2005;289:L685–L695.
37. Smith LS, Zimmerman JJ, Martin TR. Mechanisms of acute respiratory distress syndrome in children and adults: a review and suggestions for future research. Pediatr Crit Care Med 2013;14:631–643.
38. Guazzi M, Phillips SA, Arena R, *et al.* Endothelial dysfunction and lung capillary injury in cardiovascular diseases. Prog Cardiovasc Dis 2015;57: 454–462.
39. Deng B, Wang CW, Arnardottir HH, *et al.* Maresin biosynthesis and identification of maresin 2, a new anti-inflammatory and pro-resolving mediator from human macrophages. PLoS ONE 2014;9:e102362.
40. Serhan CN, Yacoubian S, Yang R. Anti-inflammatory and proresolving lipid mediators. Annu Rev Pathol 2008;3:279–312.
41. Serhan CN. Pro-resolving lipid mediators are leads for resolution physiology. Nature 2014;510:92–101.
42. Serhan CN, Chiang N, Van Dyke TE. Resolving inflammation: dual anti-inflammatory and pro-resolution lipid mediators. Nat Rev Immunol 2008;8:349–361.
43. Chiang N, Serhan CN, Dahlen SE, *et al.* The lipoxin receptor ALX: potent ligand-specific and stereoselective actions *in vivo*. Pharmacol Rev 2006;58:463–487.
44. Lavrova EA, Nikolaeva SD, Fok EM, *et al.* Lipopolysaccharide E. coli inhibits the arginine-vasotocin-induced increase of osmotic water permeability in the frog urinary bladder. Ross Fiziol Zh Im I M Sechenova 2009;95:215–224.
45. Matthay MA. Resolution of pulmonary edema. Thirty years of progress. Am J Respir Crit Care Med 2014;189:1301–1308.
46. Malik B, Price SR, Mitch WE, *et al.* Regulation of epithelial sodium channels by the ubiquitin–proteasome proteolytic pathway. Am J Physiol Renal Physiol 2006;290:F1285–F1294.
47. Soundararajan R, Melters D, Shih IC, *et al.* Epithelial sodium channel regulated by differential composition of a signaling complex. Proc Natl Acad Sci USA 2009;106:7804–7809.
48. Lee IH, Dinudom A, Sanchez-Perez A, *et al.* Akt mediates the effect of insulin on epithelial sodium channels by inhibiting Nedd4-2. J Biol Chem 2007;282:29866–29873.
49. Mattes C, Laube M, Thome UH. Rapid elevation of sodium transport through insulin is mediated by AKT in alveolar cells. Physiol Rep 2014;2:e00269.
50. Lang F, Gorlach A, Vallon V. Targeting SGK1 in diabetes. Expert Opin Ther Targets 2009;13:1303–1311.
51. Snyder PM, Olson DR, Kabra R, *et al.* cAMP and serum and glucocorticoid-inducible kinase (SGK) regulate the epithelial Na(+) channel through convergent phosphorylation of Nedd4-2. J Biol Chem 2004;279:45753–45758.
52. Zhou R, Snyder PM. Nedd4-2 phosphorylation induces serum and glucocorticoid-regulated kinase (SGK) ubiquitination and degradation. J Biol Chem 2005;280:4518–4523.
53. Gille T, Randrianarison-Pellan N, Goolaerts A, *et al.* Hypoxia-induced inhibition of epithelial Na+channels in the lung. Role of Nedd4-2 and the ubiquitin–proteasome pathway. Am J Respir Cell Mol Biol 2014;50: 526–537.
54. Yang LM, Rinke R, Korbmacher C. Stimulation of the epithelial sodium channel (ENaC) by cAMP involves putative ERK phosphorylation sites in the C termini of the channel's beta- and gamma-subunit. J Biol Chem 2006;281:9859–9868.